

# Self-lubricating nanoparticles: self-organization into 3D-superlattices during a fast drying process†

Takashi Nishio,<sup>a</sup> Kenichi Niikura,<sup>\*b</sup> Yasutaka Matsuo<sup>bc</sup> and Kuniharu Ijro<sup>\*bc</sup>

Received 30th August 2010, Accepted 8th October 2010

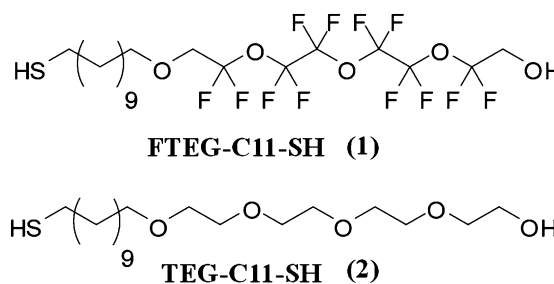
DOI: 10.1039/c0cc03538f

**Fluorinated tetraethylene glycol-stabilized Au nanoparticles (FTEG-AuNPs) were well-dispersed in general polar organic solvents, such as methanol (MeOH) and THF. The cast film of FTEG-AuNPs on a TEM grid and a glass substrate was found to form a highly ordered 3D-superlattice assembly, whereas tetraethylene glycol-stabilized AuNPs (TEG-AuNPs) provide an amorphous AuNP aggregation. These data indicate that the fluorine feature on the surface of the FTEG-AuNPs is critical for the nanostructured assembly.**

The periodic array of metal and semiconductor nanoparticles (nanoparticle superlattices) has been of great interest to researchers in a variety of fields.<sup>1</sup> These array structures have applications ranging from catalysis<sup>2</sup> to chemical sensors,<sup>3</sup> antireflection films and photonic materials.<sup>4</sup> Nanoparticle superlattices have been made by a variety of techniques, including the cross-linking of nanoparticles using template molecules,<sup>5</sup> the Langmuir–Blodgett technique,<sup>6</sup> layer-by-layer (LbL) deposition<sup>7</sup> and the self-organization method.<sup>8</sup> The self-organization method is mainly based on a simple drying process after nanoparticle solution evaporation. One of the key factors in creating highly ordered self-assembling superlattices is the slow and regulated evaporation rate of the solvent.<sup>9</sup> Therefore, low-volatile solvents, such as toluene or chlorobenzene, have been often used.<sup>10</sup> Furthermore, a large excess of stabilizer, such as surfactants and polymers, have to be added to the colloidal cast solution to obtain superlattices.<sup>11</sup> However, the drying process under these conditions is time consuming and not suitable for wet-processes (*e.g.*, inkjet printing), which would be a powerful technique applicable to superlattices for electronic, sensing and photonic devices.

Alternatively, previous theoretical analyses and simulations imply that control of particle–particle interactions by the chemical modification on the surface of nanoparticles offers another strategy for particle arrangement.<sup>12</sup> Weak interparticle interactions are important to the formation of a highly ordered array in that they prevent amorphous aggregation prior to the formation of a thermodynamically stable, close-packed structure. However, no chemical approaches to reduce

the particle–particle interactions have yet been developed. Thus, we focused on the fluorinate modification of nanoparticles since the fluorinated surface is expected to provide a low-friction property to the nanoparticles. In this study, we newly synthesized FTEG-C11-SH **1** as a capping reagent for gold nanoparticles and subsequently prepared FTEG-stabilized Au nanoparticles (FTEG-AuNPs) as the building blocks of highly ordered nanostructures. Nanoparticles protected by perfluorinated alkylthiols have been previously reported; however, these papers did not focus on their friction property, and these nanoparticles can only be dispersed in fluorinated solvents, thus their use and applications are limited due to their poor solubility.<sup>13</sup>



Perfluoroether derivatives are known lubricant materials and have been used in many applications, such as the magnetic hard disk industry, and in MEMS.<sup>14</sup> FTEG is a derivative in which the hydrogen of tetraethyleneglycol is substituted for fluorine and, because of its good solubility in several polar organic solvents, FTEG-stabilized nanoparticles were expected to be well-dispersed in various organic solvents while maintaining their fluorine feature. We, therefore, investigated their dispersity in organic solvents and observed their drying-mediated self-assembly properties on solid substrates using scanning transmission electron microscopy (STEM) and AFM for comparison with those of non-fluorinated TEG-stabilized nanoparticles.

The synthetic procedures for FTEG-C11-SH **1** are described in ESI.† In order to clarify the effect of surface fluorination, the hydrocarbon-based TEG compound **2** was also prepared according to the previous literature.<sup>15</sup> An aqueous dispersion of citric acid-protected AuNPs (20 nm in the core diameter) was concentrated by centrifugation and then added into 10 mM of compound **1** or **2**, followed by vigorous stirring for 2 days. The surface-modified nanoparticles were then purified by multiple centrifugations to remove excess thiol compounds. FTEG-AuNPs ( $1.0 \times 10^{13}$  particles  $\text{ml}^{-1}$ ,  $0.8 \text{ mg ml}^{-1}$ ) were soluble in general organic solvents, such as alcohols (*e.g.*, MeOH, EtOH), THF and acetonitrile, but insoluble in low polarity solvents, such as toluene and  $\text{CH}_2\text{Cl}_2$ , and highly polar solvents such as water (Solubility in solvents is summarized in ESI†).

<sup>a</sup> Department of Chemistry, Graduate School of Science, Hokkaido University, N10W8, Sapporo 060-0810, Japan.

<sup>b</sup> Research Institute for Electronic Science, Hokkaido University, N21W10, Sapporo 001-0021, Japan.  
E-mail: kniikura@poly.es.hokudai.ac.jp; Fax: +81 11-706-9344;  
Tel: +81 11-706-9344

<sup>c</sup> JST, CREST, N21W10, Sapporo 001-0021, Japan.

† Electronic supplementary information (ESI) available: Synthetic procedure for FTEG-C11-SH **1**, solubility, absorption spectra and DLS analysis of FTEG-AuNPs, AFM image of a cast film of 20 nm FTEG-AuNPs on the hydrophilic glass substrate. See DOI: 10.1039/c0cc03538f

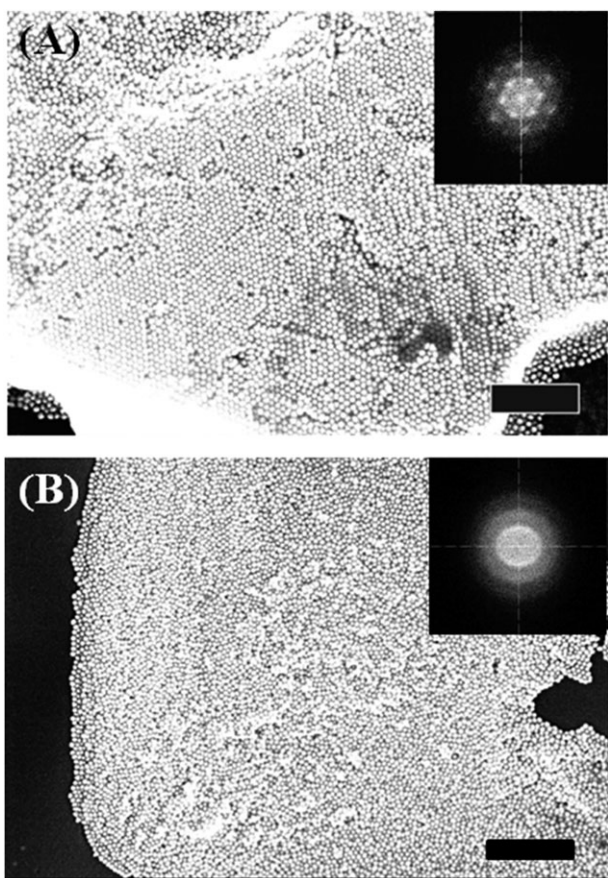


**Fig. 1** STEM images of cast-films of AuNPs (core diameter: 20 nm) on the TEM grid from methanolic solution. (A) FTEG-AuNPs, (B) TEG-AuNPs. The insets show the diffraction pattern obtained by Fourier transformation of STEM image. Scale bar: 300 nm.

The hydrodynamic diameter distribution of FTEG-AuNPs in alcohol was measured by dynamic light scattering (DLS) to give an average diameter of 20.1 nm. Moreover, FTEG-AuNPs showed a plasmon peak at *ca.* 525 nm in ethanol, which is similar to that of citrate-stabilized AuNPs in an aqueous solvent (see ESI†). Therefore, it is apparent that FTEG molecules **1** effectively stabilized Au nanoparticles in solution without aggregation.

STEM images were taken for a cast film of FTEG-AuNPs dispersed in MeOH ( $5.0 \times 10^{13}$  particles  $\text{ml}^{-1}$ ,  $4 \text{ mg ml}^{-1}$ ) on carbon-coated TEM grids (Fig. 1). A hexagonal-packed and layered structure (3D-supperlattice) was observed over a wide area ( $\sim 10 \mu\text{m}$ ). In the case of TEG-AuNPs, we were not able to observe a highly arranged 3D structure in the cast film under the same evaporation conditions as these used for the FTEG-AuNPs. This indicates that the fluorination on the nanoparticle surface must be responsible for the observed self-assembly. Fig. 2A gives a dark field TEM mode image of a three-layered region of 20 nm FTEG-AuNPs. The difference in contrast between the two background layers and the upper white layer allows us to assign each nanoparticle to its appropriate layer and conclude that the FTEG-AuNPs are assembled in a face-centered cubic (fcc)-type superlattice. Fig. 2B shows a graphic illustration clarifying the three-layered arrangement of the nanoparticle layer can be estimated at 1.5 nm, which is

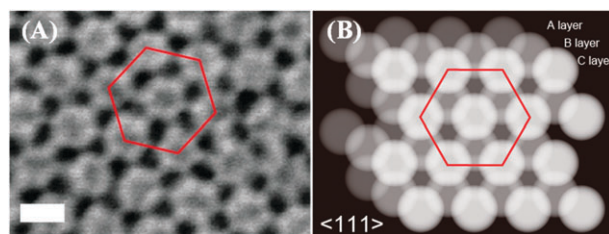


**Fig. 2** The three-layered region in the FTEG-AuNPs 3D-superlattice (20 nm in diameter). (A) STEM image of the three-layered region viewed along the  $\langle 111 \rangle$  axis of the face-centered cubic (fcc) of the 3D-superlattice, and (B) the corresponding schematic representation. Scale bar: 20 nm.

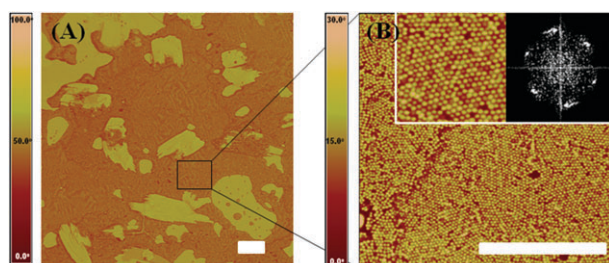


**Fig. 3** AFM images (phase mode) of a 20 nm FTEG-AuNP cast film deposited on a hydrophobic glass substrate. (A) Brown regions show multilayered superlattices formed on the substrate. The bright regions show the bare glass substrate. (B) The bright regions show nanoparticles. The left inset shows a magnified image ( $500 \times 500 \text{ nm}$ ). The right inset shows the diffraction pattern obtained by Fourier transformation of the magnified AFM image. Scale bar:  $1 \mu\text{m}$ .

shorter than the theoretical molecular length of a FTEG molecule **1** (*ca.* 3 nm). This means that the capping thiol molecules apparently either tilt or interdigitate with a molecule on the opposite side. Fig. 3 shows an AFM image of a cast film of 20 nm FTEG-AuNPs on a siliconized hydrophobic glass substrate. We can see the multilayer 3D-superlattice in which 20 nm FTEG-AuNPs are arranged over a large area. On the other hand, on the hydrophilic substrate (clean glass), we observed the formation of an unassembled monolayer fraction of nanoparticles (see ESI†). As the siliconized hydrophobic glass substrate has a low surface tension and a dewetting property for MeOH, the height of the droplets can be maintained, resulting in the successful growth of 3D lattices.

Finally, we tried to construct superlattices composed of 5 nm FTEG-AuNPs by a cast from MeOH; however, no 3D-superlattice was produced, which is contrary to the readily formed superlattices observed with 20 nm FTEG-AuNPs. However, lowering the evaporation rate by changing the solvent from MeOH to isopropanol, whose relative evaporation rate is 1.9 times slower than that of MeOH, gave a 3D-superlattice (Fig. 4). This indicates that FTEG-modification is effective in the formation of superlattices even for nanoparticles of several nanometres in size when the proper solvent is used.

We considered that the well-ordered nature of the FTEG-AuNPs resulted from the “self-lubricating” property (low particle–particle friction) of the fluorinated surface. After the particle is fixed by the capillary force of the liquid thin film on the substrate, it is necessary to shift from an amorphous

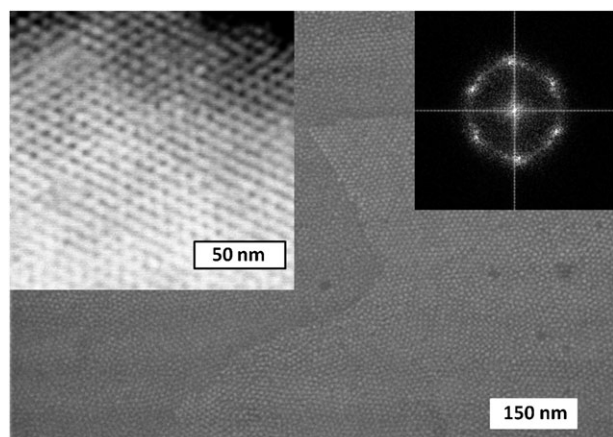


**Fig. 4** STEM image of a cast-film of FTEG-AuNPs (core diameter: 5 nm) dissolved in isopropanol. SEM mode overview and dark field mode detail (left inset) images were shown. The right small inset shows a Fourier transformation image of the overview image.

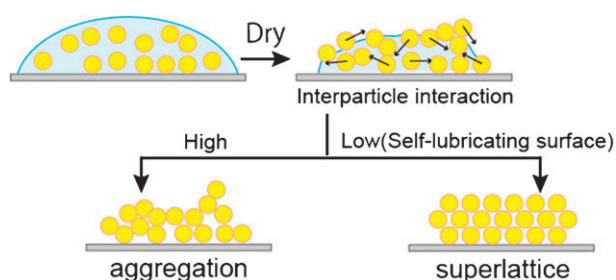


**Fig. 5** Hypothetical mechanism for the formation of the close-packed structure of FTEG-AuNPs during the fast drying process. The arrows indicate the motion (rearrangement) of nanoparticles in the concentrated state due to strong lubricating property of FTEG-AuNPs.

state to a crystal state. To reach a thermodynamically stable, close-packed state, each nanoparticle needs to move freely during the final stage of solvent drying (Fig. 5). The fluorinated nanoparticles provide weak particle–particle interactions, thus there is a low energetic barrier to the rearrangement of packing during the drying process, leading to thermodynamically stable, close-packed 3D structures within a short period. Experiments to provide the evidence of our hypothesis are currently underway.

In summary, we have shown the synthesis of FTEG-stabilized AuNPs that are dispersed homogeneously in polar organic solvents and are stable even at high concentrations.

Casting of the dispersion gave a 3D-superlattice with a highly regular hexagonal-packed structure, whereas non-fluorinated TEG-AuNPs produced only amorphous aggregations under the same conditions. Since this method did not need conventional slow-evaporation procedure, the FTEG-coating of nanoparticles afford a useful and versatile approach to the production of various metal nanoparticle superlattices compatible with the use of a simple wet-process, such as spin coating or inkjet printing.

A part of this work was conducted at Hokkaido Innovation through Nanotechnology Support (HINTS), supported by "Nanotechnology Network JAPAN" Program of the Ministry of Education, Culture, Sports, Science and Technology (MEXT), Japan and the OPEN FACILITY, Hokkaido University Sousei Hall. This study was supported in part by Research Fellowships of the Japan Society for the Promotion of Science for Young Scientists.

## Notes and references

- (a) C. P. Collier, T. Vossmeier and J. R. Heath, *Annu. Rev. Phys. Chem.*, 1998, **49**, 371–404; (b) B. L. V. Prasad, C. M. Sorensen and K. J. Klabunde, *Chem. Soc. Rev.*, 2008, **37**, 1871–1883; (c) D. V. Talapin, *ACS Nano*, 2008, **2**, 1097–1100.
- J. Park, E. Kang, S. Son, H. Park, M. Lee, J. Kim, K. Kim, H. J. Noh, J. H. Park, C. Bae, J. G. Park and T. Hyeon, *Adv. Mater.*, 2005, **17**, 429–434.
- (a) E. Shibu, M. Habeeb Muhammed, K. Kimura and T. Pradeep, *Nano Res.*, 2009, **2**, 220–234; (b) E. S. Shibu, K. Kimura and T. Pradeep, *Chem. Mater.*, 2009, **21**, 3773–3781.
- (a) K. Hosoki, T. Tayagaki, S. Yamamoto, K. Matsuda and Y. Kanemitsu, *Phys. Rev. Lett.*, 2008, **100**, 207404; (b) C. Rockstuhl and T. Scharf, *J. Microsc. (Paris)*, 2008, **229**, 281–286; (c) A. L. Rogach, *Angew. Chem., Int. Ed.*, 2004, **43**, 148–149.
- (a) S. I. Lim and C.-J. Zhong, *Acc. Chem. Res.*, 2009, **42**, 798–808; (b) S. Y. Park, A. K. R. Lytton-Jean, B. Lee, S. Weigand, G. C. Schatz and C. A. Mirkin, *Nature*, 2008, **451**, 553; (c) D. Nykypanchuk, M. M. Maye, D. van der Lelie and O. Gang, *Nature*, 2008, **451**, 549.
- M. Achermann, M. A. Petruska, S. A. Crooker and V. I. Klimov, *J. Phys. Chem. B*, 2003, **107**, 13782–13787.
- (a) J. Cho and F. Caruso, *Chem. Mater.*, 2005, **17**, 4547–4553; (b) M.-H. Lin, H.-Y. Chen and S. Gwo, *J. Am. Chem. Soc.*, 2010, **132**, 11259–11263.
- (a) E. Rabani, D. R. Reichman, P. L. Geissler and L. E. Brus, *Nature*, 2003, **426**, 271–274; (b) H. Yao, H. Kojima, S. Sato and K. Kimura, *Langmuir*, 2004, **20**, 10317–10323; (c) S. He, J. Yao, P. Jiang, D. Shi, H. Zhang, S. Xie, S. Pang and H. Gao, *Langmuir*, 2001, **17**, 1571–1575; (d) M. Grzelczak, J. Vermant, E. M. Furst and L. M. Liz-Marzán, *ACS Nano*, 2010, **4**, 3591–3605; (e) A. Dong, J. Chen, P. M. Vora, J. M. Kikkawa and C. B. Murray, *Nature*, 2010, **466**, 474–477.
- (a) T. P. Bigioni, X.-M. Lin, T. T. Nguyen, E. I. Corwin, T. A. Witten and H. M. Jaeger, *Nat. Mater.*, 2006, **5**, 265–270; (b) C. J. Kiely, J. Fink, M. Brust, D. Bethell and D. J. Schiffrin, *Nature*, 1998, **396**, 444–446.
- E. V. Shevchenko, D. V. Talapin, A. L. Rogach, A. Kornowski, M. Haase and H. Weller, *J. Am. Chem. Soc.*, 2002, **124**, 11480–11485.
- X. M. Lin, H. M. Jaeger, C. M. Sorensen and K. J. Klabunde, *J. Phys. Chem. B*, 2001, **105**, 3353–3357.
- (a) M. Fujita, H. Nishikawa, T. Okubo and Y. Yamaguchi, *Jpn. J. Appl. Phys.*, 2004, **43**, 4434–4442; (b) M. Hu, S. Chujo, H. Nishikawa, Y. Yamaguchi and T. Okubo, *J. Nanopart. Res.*, 2004, **6**, 479–487.
- (a) T. Yonezawa, S. Onoue and N. Kimizuka, *Adv. Mater.*, 2001, **13**, 140–142; (b) T. Yonezawa, S.-y. Onoue and N. Kimizuka, *Langmuir*, 2001, **17**, 2291–2293; (c) A. Dass, R. Guo, J. B. Tracy, R. Balasubramanian, A. D. Douglas and R. W. Murray, *Langmuir*, 2008, **24**, 310–315.
- (a) A. J. Gellman, *Curr. Opin. Colloid Interface Sci.*, 1998, **3**, 368–372; (b) Y. Yun, E. Broitman and A. J. Gellman, *Langmuir*, 2006, **23**, 1953–1958.
- K. Niikura, T. Nishio, H. Akita, Y. Matsuo, R. Kamitani, K. Kogure, H. Harashima and K. Ijiri, *ChemBioChem*, 2007, **8**, 379–384.